Cement and Concrete Research 39 (2009) 600–609

Contents lists available at ScienceDirect

Cement and Concrete Research

journal homepage: http://ees.elsevier.com/CEMCON/default.asp

# Study of mineralogy and leaching behavior of stabilized/solidified sludge using differential acid neutralization analysis
## Part I: Experimental study

O. Peyronnard [a,*], M. Benzaazoua [b], D. Blanc [a], P. Moszkowicz [a]

[a] LGCIE Site Carnot, INSA-Lyon, 9 rue de la Physique, Villeurbanne, F 69621, France
[b] UQAT, 445 Blvd de l'Université, Rouyn-Noranda, Québec, Canada J9X 5E4

ARTICLE INFO

*Article history:*
Received 29 October 2007
Accepted 27 March 2009

*Keywords:*
Waste management
Characterization
Stability
Fly ash
Portland cement

ABSTRACT

In this work, differential acid neutralization analysis, chemical analysis of selected leachates and mineralogical study (XRD and SEM-EDS) are combined to investigate the relationship between mineralogy and leaching behavior of hydroxide sludge doped in Zn and Cr stabilized/solidified by hydraulic binders. The leaching behavior of stabilized hydroxide sludge is controlled by the dissolution of portlandite ($pH \sim 12$) followed by the dissolution of AFt/AFm and hydrogarnets (pH between 12 and 10) and finally the dissolution of ettringite and of the siliceous matrix of C–S–H ($pH < 10$). The zinc behavior is independent of the main components and is controlled by the dissolution of calcium hydroxizincate and its reprecipitation as hydroxyde or its adsorption on C–S–H. Chromium release is linked to the sulfate one due to a substitution in AFt/AFm phases.

The proposed combination of tests is highly pertinent to establish the links between mineralogy and leaching behavior. Nevertheless, the hypotheses formulated are insufficient to implement a behavioral model to describe the leaching behavior.

## 1. Introduction

During their storage, wastes which have been stabilized/solidified by hydraulic binders can react with aqueous media that induce a certain weathering of the solid matrix and a possible release of the pollutants (heavy metals) that they contain. To make sure of the absence of risk for the environment, waste storage scenarios should be environmentally assessed. These assessments require a determination of the leaching behavior of the stabilized/solidified wastes. Legislations, for the storage or the reuse of mineral wastes, are generally based on "conformity" tests that are interpreted with regard to limiting values for toxic species: if pollutant concentrations in leachates are below the limits, the behavior is considered as satisfactory. Nevertheless, such leaching tests results can't be considered as representative of realistic pollutants mobilization because of exposition conditions far from real ones. For example, due to their short leaching period, most of these tests are suitable for estimating the release of highly soluble species but can't exhibit the mobilization of pollutants having a behavior dependant of the leaching conditions (e.g. pH, Eh…) or linked to the solid matrix evolution (e.g. sorption). In the last years, an approach based on the estimation of the leaching behavior in specified conditions appears, in particular in European countries [1,2]. This approach is based on the extrapolation of various leaching tests (acid neutralization capacity, influence of pH on elements release, leachable fraction…) to realistic conditions in order to predict to the pollutants mobilization in the envisaged scenario. The main benefit of such approaches is that the risk assessment is based on the comprehension of the mechanisms controlling the pH evolution and the mobilization of the metals. It, also takes into account the specificities of the scenario.

With this in mind, modeling and numerical simulations became essential tools for environmental risk assessment. Indeed geochemical models were shown to be able to predict the leaching from inorganic wastes, in particular cementitious materials [3]. Being based on the equilibrium laws between solid and liquid phases, theses models require a minimal knowledge of the mineralogical composition of the studied material. Therefore mineralogical analyses were added to leaching tests to characterize the wastes. X-ray diffractometry (XRD), and thermal analysis inform on the nature of the main mineral phases. Electronic microscopy (SEM-EDS) can be used to localize elements; in particular pollutants. Nevertheless, mineralogical analyses have some limitations to determine the speciation of metals, and other traces elements, in solidified wastes matrixes:

- XRD only permits the identification of well crystallized phases whereas cementitious matrixes are mainly composed of amorphous minerals;
- SEM-EDS resolution is insufficient to permit a fine identification of hydrated cement phases and the localizations of pollutants in the matrixes.

---

[*] Corresponding author. Tel.: +33 4 72 43 88 41; fax: +33 4 72 43 87 17.
*E-mail address:* olivier.peyronnard@uqat.ca (O. Peyronnard).

0008-8846/$ – see front matter © 2009 Elsevier Ltd. All rights reserved.
doi:10.1016/j.cemconres.2009.03.016

The differential acid neutralization analysis, proposed by Glass and Buenfeld [4], permits a mineralogical interpretation of the leaching behavior. The derivation of the titration curve ($dH^+/dpH$) transforms it into a spectrum of discrete peaks resulting from the dissolution of a particular mineral present in the matrix. Thus, this differential analysis should permit the identification of the hydrated cement phases governing the leaching behavior. Moreover, the area below each peak represents to the acid consumption needed for the dissolution of the related phase [4]. Therefore, this differential analysis permits a semi-quantitative determination of the cementitious phases present in the matrix.

However, hydrated cement phases' stability is influenced by leachate composition and interactions (interferences and/or precipitation phenomenon) with other mineral phases [5,6]. So identification of the phase responsible for each peak is fairly complex without a minimum knowledge of the material mineralogy [4]. Leachate chemistry can provide a substantial help [7–9]. For each peak, the release of the main elements (e.g. Ca, Si, Al, Fe, $SO_4^{2-}$) informs on the nature of the dissolving mineral. The mobilization of pollutants (e.g. Cr, As, Pb, Zn…) informs on their hosts and retention mechanisms. The main evolutions of the leachates compositions occur during the dissolution of minerals. Therefore, only the leachates obtained before and after each peak are required to identify the dissolving minerals (phases composing the matrix) and the retention mechanisms of metals [9].

This two parts paper deals with the characterization and the modeling of the leaching behavior of stabilized/solidified sludge doped with zinc and chromium. In this first part, an experimental study, coupling differential acid neutralization, chemical analysis of selected leachates and a mineralogical study (SEM-EDS and XRD), was implemented to establish the links between mineralogy and leaching behavior. In the second part, we'll propose to use geochemical modeling to facilitate the interpretation of experimental results and the setting of a behavioral model.

To improve the identification of the cementitious hydrates and the mechanisms of pollutants retention/release, some modifications were made on the experimental protocol (conductivity measurement and selected leachates analysis) and the mathematical treatment (derivative calculations) proposed by Glass and Buenfeld. The results were, then, confronted to a mineralogical study (SEM-EDS and XRD) to elaborate a conceptual model of leaching of stabilized/solidified hydroxide sludge. This study was performed on synthetic hydroxide sludge stabilized/solidified by hydraulic binders composed of ordinary Portland cement and coal fly ashes. Comparison between stabilized sludge and control samples were made to study the influence of sludge and/or fly ash on the hydration of Portland cement.

## 2. Materials and methods

### 2.1. Materials

Hydroxide sludge is a waste resulting from the pollution control of bath used for electrolytic surfaces treatment of metals and alloys. This sludge contains typically various metals and, consequently, consists in a complex matrix. In order to reduce this complexity, the authors have chosen to work on sludge containing iron, zinc and hexavalent chromium synthesized at the laboratory (Table 1). To do this, an acidic solution containing zinc, iron and hexavalent chromium were neutralized by sodium hydroxide. Nevertheless, because of material limitation, all the necessary sludge couldn't be prepared in one batch. So we chose to dry it to avoid any differences between sludge coming from the different batches due to their potential chemical or mineralogical evolution.

**Table 1**
Composition of Portland cement, coal fly ashes and hydroxide sludge (wt.%).

| | OPC | PFA | Dried sludge |
|---|---|---|---|
| CaO | 63% | 3% | – |
| $SiO_2$ | 21% | 50% | – |
| $Al_2O_3$ | 7.3% | 29% | – |
| $Fe_2O_3$ | 5.5% | 8.5% | 37.1% |
| MgO | 0.9% | 3% | – |
| $Na_2O$ | 1.5% | 0.7% | 15.8% |
| $K_2O$ | 2.3% | 4.5% | 0.6% |
| ZnO | 0.1% | – | 15.2% |
| $CrO_4^{2-}$ | – | – | 0.7% |
| $SO_4^{2-}$ | 1.9% | 0.6% | 4.4% |
| $Cl^-$ | 0.1% | 0.04% | 6.2% |
| $NO_3^-$ | – | – | 3.8% |
| $PO_4^{3-}$ | 0.3% | 0.25% | 16.2% |

**Table 2**
Formulations of the four studied materials.

| Ref. | OPC | PFA | Dried sludge | Water |
|---|---|---|---|---|
| OPC | 100 g | 0 | 0 g | 40 mL |
| OPC-PFA | 50 g | 50 g | 0 g | 40 mL |
| OPC–S | 86.8 g | 0 | 13.2 g | 46 mL |
| OPC–PFA–S | 43.4 g | 43.4 g | 13.2 g | 48 mL |

Two different binders (Table 1) were used to stabilize dried sludge: a pure Ordinary Portland Cement (OPC, CEM I with regard to European standard) and a mix of 50% of OPC and 50% of class F Fly Ashes (PFA, Surschiste's Silicoline®). Four distinct materials were analyzed (Table 2): two blanks (OPC and OPC–PFA) corresponding to the two binders used and two stabilized sludge (OPC–S and OPC–PFA–S). The sludge load in OPC–S and OPC–PFA–S was determining during preliminary tests [10] that show that higher loads highly inhibit the binders' hydration. Control samples (OP and OPC–PFA) were prepared with a water/cement (w/c) ratio equal to 0.4. An increase of the mixing water amount was required for the materials containing sludge (OPC–S and OPC–PFA–S) due to its water demand (Table 2). It must be noted, that this w/c increase will increase the porosity of the matrix and, thereby intensify the diffusion process during leaching.

The four cement pastes of stabilized/solidified sludge were cured for 28 days in $4\times4\times16$ cm$^3$ mold in air tight conditions (sealed plastic bags) to avoid any water evaporation and carbonation of the mortars. At the end of the cure, hydration reactions were stopped by immersion in acetone during 24 h and drying at 40 °C until stabilization of their mass [13]. One $4\times4\times4$ cm$^3$ cubic block was cut from each paste in order to perform a sequential monolithic leaching test. The remaining parts were crushed to a particle size inferior of 1 mm for the differential acid neutralization analysis tests.

### 2.2. Methods

#### 2.2.1. Differential acid neutralization analysis

For each material, the acid neutralization data were obtained from a series of 20 batch tests. In each batch, 60 ml of a nitric acid solution (variable concentration) is added to 12.5 g of powdered material (L/S = 4 L/kg). The acid nitric concentrations (0 to 3.8 mol/L) were implemented in order to obtain a pH evolution from natural pH (pH of equilibrium of the solid with pure water) to a pH between 9 and 10. Tests were performed in a rotary shaker for a period of 8 days to reach the total equilibrium between the liquid and solid phases. Preliminary investigations show that after 8 days, the leachate pH remains constant [10]. Therefore, the equilibrium between the solid matrix and the aqueous solution can be considered as reached. Leachates were then filtered to 0.45 µm on a Büchner filter and conductivity and pH were measured. For each material, 5 to 7 leachates were analyzed by ICP AES for Ca, Al, Si, Fe, Cr, Zn, Mg, K and Na (norm NF EN ISO 11885). Sulfate and chloride were analyzed by ion chromatography (norm NF EN ISO 10304-2). Concentrations are given with an uncertainty of 10%. Analyses were focalized on the leachates corresponding to the end of a dissolution.

The differential analysis used in this work slightly differs from those proposed by Glass and Buenfeld [4]. The derivative ($dH^+/dpH$) is calculated using a centered difference scheme (Eq. (1)); explicit and implicit schemes were used for the extrema Eqs. (2) and (3). To smooth spectra, a point was added between each two experimental points by linear interpolation.

$$\left(\frac{d\mathrm{H}^+}{d\mathrm{pH}}\right)_i = \frac{\mathrm{H}^+_{i+1} - \mathrm{H}^+_{i-1}}{\mathrm{pH}_{i+1} - \mathrm{pH}_{i-1}} \tag{1}$$

$$\left(\frac{d\mathrm{H}^+}{d\mathrm{pH}}\right)_1 = \frac{\mathrm{H}^+_{2} - \mathrm{H}^+_{2}}{\mathrm{pH}_{2} - \mathrm{pH}_{2}} \tag{2}$$

$$\left(\frac{d\mathrm{H}^+}{d\mathrm{pH}}\right)_N = \frac{\mathrm{H}^+_{N} - \mathrm{H}^+_{N-1}}{\mathrm{pH}_{N} - \mathrm{pH}_{N-1}} \tag{3}$$

with:

| | |
|---|---|
| $i$ | index of the batch |
| $N$ | total number of batches |

Each dissolution and precipitation occurring during the acid titration results in an increase or decrease of the leachates' content of solute and so, of its conductivity. Therefore, we also add to Glass's protocol the measure of the conductivity of the leachates. Its evolutions were interpreted in terms of conductivity evolution induced by a unit pH change (dC/dpH). The same mathematical treatment was used to plot the conductivity spectra.

### 2.2.2. Sequential monolithic leaching test

The 4×4×4 $cm^3$ cubic blocks were submitted to a sequential batch leaching test. This test consists in studying the dynamic of the leaching by renewing the leaching solution after predetermined periods of leaching (6, 18 and 24 h, 2, 4, 8, 16 and 32 days). The leaching agent used was demineralized water, introduce at a liquid/solid ratio of 10 L/kg. The homogeneity of the leachate was guaranteed by a mixing with a magnetic stirrer. Once the monolith leaching test ended, the leached monoliths were dried at 40 °C until stabilization of their mass. A section was cut from each leached monolith to be observed by SEM.

The results of leachates analyses are not presented in this paper because they can hardly be interpreted to characterize the mineralogy of stabilized/solidified sludge or the heavy metals retention/mobilization mechanisms. Detailed results can be found be found in Peyronnard's PhD [10].

### 2.2.3. SEM-EDS observations

SEM observations were made using a JEOL's 840 A LGS microscope coupled to a PGT's EDS system. Observations were conducted at a working distance of 12 mm with an acceleration voltage of 20 keV and a current between $10^{-9}$ and $10^{-6}$ A. The observed sections were cut, using a manual wire saw, perpendicularly to the leaching surface of leached monolith and prepared using the following protocol:

- Void impregnating in a epoxy resin by cold polymerization;
- Dry polishing with sand paper having a decreasing grading (80–400 to 800–1000);
- Polishing with a 3 µm diamond disk with a non aqueous lubricant;
- Cleaning with absolute alcohol;
- Coating with a gold layer of around 18 nm thick using a SCD 040 metalizer.

The cores of the sections were not subjected to the leaching mechanism. Therefore, they were considered as representative of the unleached materials.

### 2.2.4. X-ray diffractometry

The unleached materials were studied by XRD using a SIEMENS's D500 diffractometer. Samples were ground to fine powders using a manual pestle. The investigations were made and for a reflection angle (2θ) between 0 and 70° with an angle step of 0.02°. Measurement time was fixed to 1 s per step. Mineral phases were identified with the help of the software EVA.

## 3. Results

### 3.1. Differential acid neutralization analysis

Titration curves (Fig. 1) show typical results with:

- a titration curve of pure cement (OPC) showing three major plateaus which is in accordance with data from literature [4,5];
- a loss of neutralization capacity for materials incorporating fly ashes and/or sludge [5].

The loss of resistance to acidification is mainly due to a decrease of the portlandite amount in pastes containing sludge and/or PFA. Indeed, for materials containing PFA, this decrease is due to pozzolanic reactions that form C–S–H from reaction of portlandite with silica coming from PFA [11]. For OPC–S, the decrease is due to the hydration inhibition caused by the zinc present in the sludge [12–14]. Actually, this inhibition induces that a lower fraction of OPC is hydrated, and thereby the amount of precipitated portlandite is lower than for pure OPC.

For each paste, plotting $dH^+/dpH$ and dC/dpH evolution as function of pH gives two very similar spectra (Fig. 2). The small differences observed are due to the variations of conductivity caused by variations of ionic contents during dissolution reactions. Therefore, the dC/dpH spectrum permits to confirm, or infirm, the presence of not well individualized peaks appearing on $dH^+/dpH$ spectrum. For example, the small peak occurring for pH between 9.9 and 9.8 on OPC–PFA $dH^+/dpH$ spectrum is confirmed by a more pronounced peak on dC/dpH spectrum.

The OPC spectrum consists of five peaks at pH around 12.4, 12.1, 11.4, 10.6 and 10.1. For pH under 10, an increase of $dH^+/dpH$ is noticed, but, the lack of data prevents the confirmation of the existence of this peak. Therefore, as suggested by Glass and Buenfeld [3], the leaching behavior of OPC is controlled by the dissolution of five mains hydrates, among portlandite at pH around 12.1, ettringite for pH between 11 and 10 and C–S–H for pH lower than 10.

The leaching behavior of OPC–S seems to be controlled by six mineral phases dissolving respectively at pH around 12.2, 11.9, 11.7, 11.4, 11.1 and 10.8. By comparison with the behavior of OPC, the peak occurring at pH equal 12.2 is attributed to the dissolution of portlandite, and those appearing for pH around 10.8 to the dissolution of ettringite. The dissolution of C–S–H probably causes the peak that occurs for pH below 10 but it can't be confirmed due to a lack of data. The minerals initiating the peaks occurring 11.1 and 11.9 can't be identified without any further investigations.

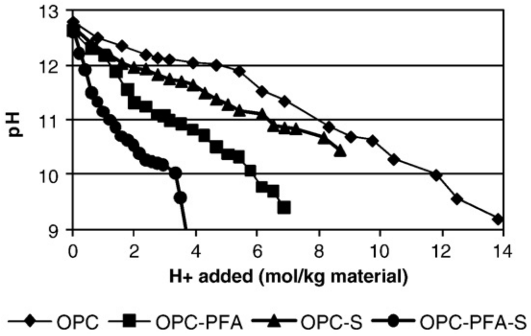

**Fig. 1.** Titration curves of the four studied materials.

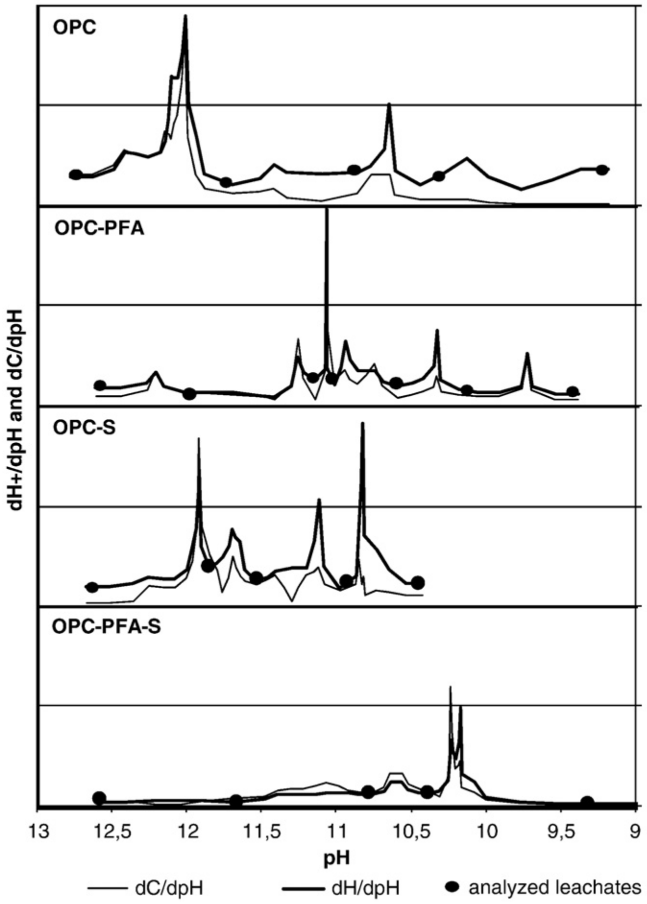

**Fig. 2.** Differential analysis spectra of the four studied materials.

The response to acidification of OPC-PFA and OPC-PFA-S is controlled by seven dissolution reactions that, respectively, occur for pH around 12.2, 11.3, 11.1, 10.9, 10.7, 10.3 and 9.7 and pH around 12, 11.4, 11.1, 10.9, 10.6, and 10.2 (double peak). The comparison with the OPC behavior permits to attribute the peaks occurring at pH around 12.2 and 12 to the dissolution of portlandite. The minerals that dissolve for pH between 10 and 11 are probably ettringite and other AFt phases. CSH are dissolved when the pH decrease below 10.

For the four studied pastes, the pH 12 peak is attributed to the dissolution of portlandite. The comparison of its intensity for the different materials highlights the decrease of portlandite amount with the adding of PFA and/or sludge: decrease of peak intensity for paste containing PFA and/or sludge. Semi-quantitative calculations, based on the area below each peaks, show that the amount of portlandite in OPC–PFA is less than the half of OPC paste one. The decrease is due to the dilution of OPC in the binder (50%) and the consumption of portlandite by pozzolanic reactions. The decrease of portlandite amount due to hydration inhibition by sludge can also be estimated. The amount of portlandite in OPC–S is about the half of pure OPC one and those of OPC–PFA–S is very low (less than the half of OPC–PFA one).

The comparison of the spectra from the different studied pastes reveals three main kinds of differences:

- Decrease/Increase in peak intensity, as seen previously for the peak caused by the dissolution of portlandite;
- Shifts of pH of minerals dissolution: for example, the peaks caused by the dissolution of ettringite occur at a pH varying from 10.1 to 10.3;
- Appearance of new peaks, for example, the peak occurring at pH around 11.7 for OPC–S but not present in OPC.

As seen for the portlandite peak, variations of intensity reflect the variations of the amount of the related hydrated phase.

The variations of the pH where the dissolution of a mineral occurs are caused by the influence of leachates composition on minerals stability. Indeed, the solutes present in the leachate can delay or favor the dissolution of minerals. For example, a high concentration in calcium tends to delay the dissolution of calcareous minerals. The solutes can also initiate dissolution reactions. For example, in the case of sulfatic attack, the high sulfates' concentration induces the dissolution of aluminates (hydrogarnets, AFm…) and the reprecipitation of aluminum and sulfates as ettringite.

Finally, appearance of new peaks can result from phases initially present in sludge or PFA and from hydration products resulting from the interaction of OPC with PFA or sludge.

### *3.2. Release of elements*

Leachates of each material were analyzed at the points shown in Fig. 2. Fig. 3 represents the release of elements among the decrease of pH. With the exception of K and Na, the release of elements is dependent on the pH. Some elements, like Al or Fe, remain weakly soluble in the studied range of pH, whereas others (Ca, Si, $SO_4^{2-}$) are highly leached (Fig. 3).

For the four materials, calcium concentration increases all along the decrease of pH due to Ca presence in most cementitious hydrates. Nevertheless, the decrease of portlandite amount observed with the adding of PFA or sludge is reflected in Ca mobilization in the first times of the acidification.

Silicon had a similar behavior for OPC, OPC–PFA and OPC–S with a slight increase of release from natural pH to a pH around 10–10.5 where a significant increase is observed. In Portland cement and OPC/PFA blend, silicon is mainly contained in C–S–H. Therefore, the observed release of silicon confirmed the attributions to C–S–H dissolution of the peaks occurring for pH below 10. It is important to note that the dissolution of C–S–H is non congruent (decalcification) and occurs gradually all along the decrease of pH. So the peaks attributed to the dissolution of C–S–H reflect the dissolution of their siliceous structure. For OPC–PFA–S, silicon appears as highly soluble at natural pH and its solubility decrease during the acidification. As seen previously, the zinc inhibits the hydration of cement. Therefore, this high release of silicon probably corresponds to the dissolution of unhydrated cement phases ($C_3S$ and $C_2S$). The decrease of silicon release with the acidification of the matrix is explained by its probable precipitation with calcium released from other hydrates.

For the four materials, the sulfate is released for pH between 10.6 and 10.2. Therefore, the mobilization of sulfate at “low” pH is controlled by a same hydrate: probably ettringite. However, for OPC–S and OPC–PFA–S, a decrease of the sulfate release is observed in the first time of acidification (pH>11.5). This behavior can be explained by the occurrence of sulfate as ettringite or gypsum: minerals which are relatively soluble in highly alkaline media. So, the sulfate is not precipitated in the same form in sludge containing materials (OPC–S and OPC–PFA-S) and in pure binders (OPC and OPC–PFA). Considering the amount of sulfates provided by sludge (Table 1), it's possible that sulfate is precipitated as ettringite in OPC–S and OPC–PFA–S and as monosulfoaluminate in OPC and OPC–PFA. Nevertheless, during acidification, monosulfoaluminate, present in OPC and OPC–PFA, is probably transformed in ettringite.

The release of aluminum remains globally relatively low on the studied range of pH, nevertheless its weak evolutions permit to establish hypothesis on the hydrated phases responsible of some peaks. For OPC, the leaching of aluminum increases a first time for pH between 12.8 and 11.5 and a second time for pH between 10.9 and 10.3. Therefore, the two relative peaks are caused by the dissolution of phases containing aluminum: AFt, AFm, hydrogarnets or other C–A–H. For OPC–PFA and OPC–S, the aluminum release reaches a maximum for a pH between 11.3

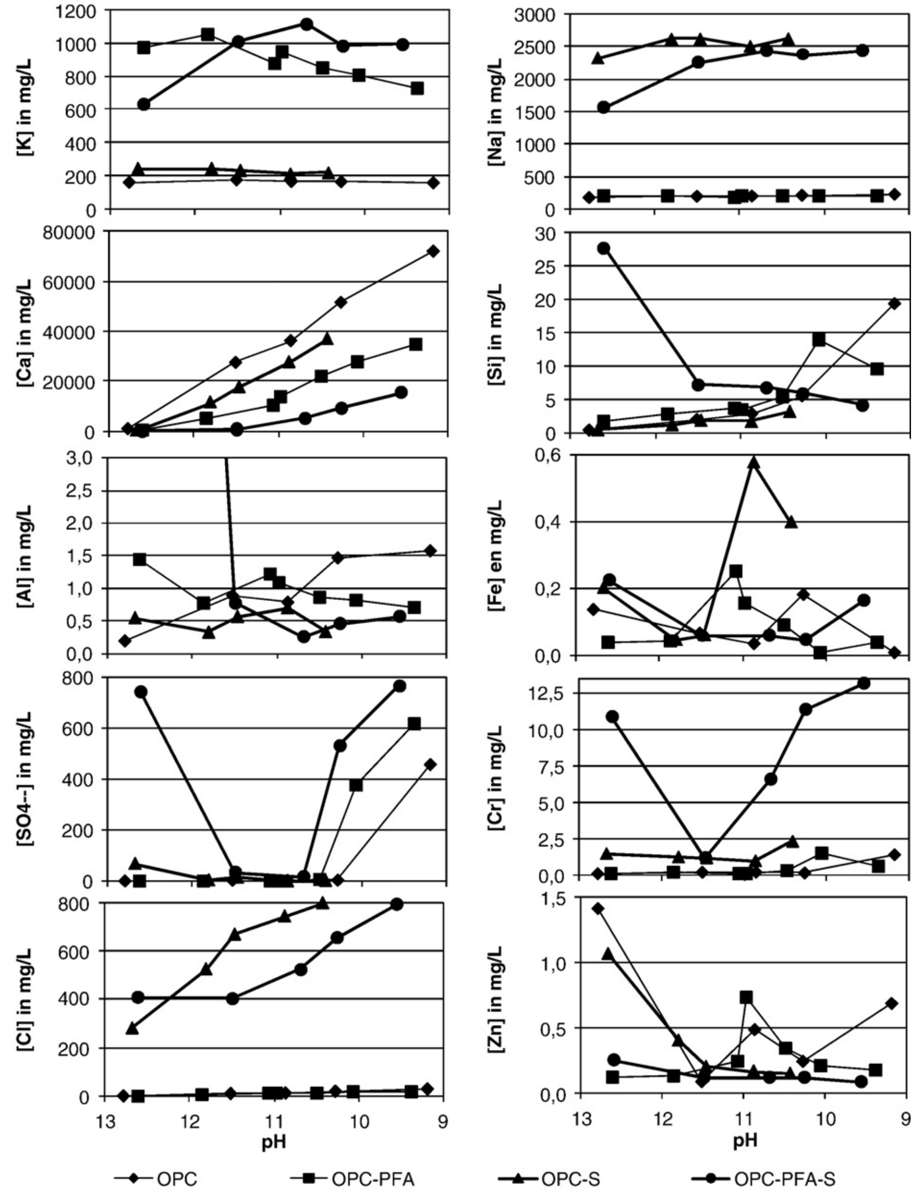

**Fig. 3.** Evolutions of the release of elements against the pH for the four materials.

and 10.8 and decreases for lower pH. So, the mobilization of aluminum is controlled by a phase dissolving for pH included between 11.3 and 10.8 followed by a reprecipitation of aluminum, probably as hydroxide (Al $(OH)_3$). For these two pastes, a slight decrease of aluminum release can also be observed in the first time of the acidification (pH between 12.7 and 11.8). For OPC–PFA–S, aluminum is highly released (25.2 mg/l) under basic conditions. Comparison between aluminum and sulfate releases tends to show a correlation for highly alkaline conditions. For lower pH, we can note that the increase of aluminum and sulfate mobilizations occur simultaneously, but the amount of aluminum released is low in regard of sulfate one. This behavior can be explained by the presence of ettringite, in OPC–PFA–S. For low pH ($<10.7$), the aluminum, liberated by the dissolution of ettringite, probably precipitates as hydroxide (Al concentration are close to those observed for (OPC–S and OPC–PFA).

As aluminum ones, iron concentrations in leachates remain weak. However, its variation permit to establish hypothesis on the origin of peaks observed on differential analysis spectra. For OPC, the leaching of iron increases between pH 10.9 and 10.3 simultaneously to an increase of aluminum release. Therefore, the related peak is caused by the dissolution of an aluminate (AFt, AFm hydrogarnets or other C–A–H) and its ferrous homolog. For OPC–PFA and OPC–S, the release of iron is linked to the peak obtained for pH around 11.3. So, this peak is probably caused by the dissolution of a ferrous AFt or AFm. In the case of OPC–PFA–S, the release of iron remains weak all along the range of pH with a higher release for highly alkaline conditions and pH down to 10.3. This behavior could be explained by the presence of iron as ferrous ettringite homolog. However the variations are too weak to attribute a peak of the differential analysis spectrum to the dissolution of a mineral containing iron.

Magnesium has a similar behavior for the four materials with an increase of leaching from pH around 10. Its release is independent of the apparition of peaks. Chloride can't be, here, considered as a soluble (element released independently of the pH) in particular for OPC–PFA–S and OPC–S. For natural pH, the release of chloride is relatively low but increases right from the start of the acid attack. Chloride could appear as Friedel's or Kuzel's salt (respectively $(CaO)_3 \cdot Al_2O_3 \cdot CaCl_2{:}10H_2O$ and $(CaO)_3 \cdot Al_2O_3 \cdot CaCl(SO_4)_{0.5}{:}10H_2O$) and their ferrite analogs [8] which dissolution have been reported for pH around 12 [15].

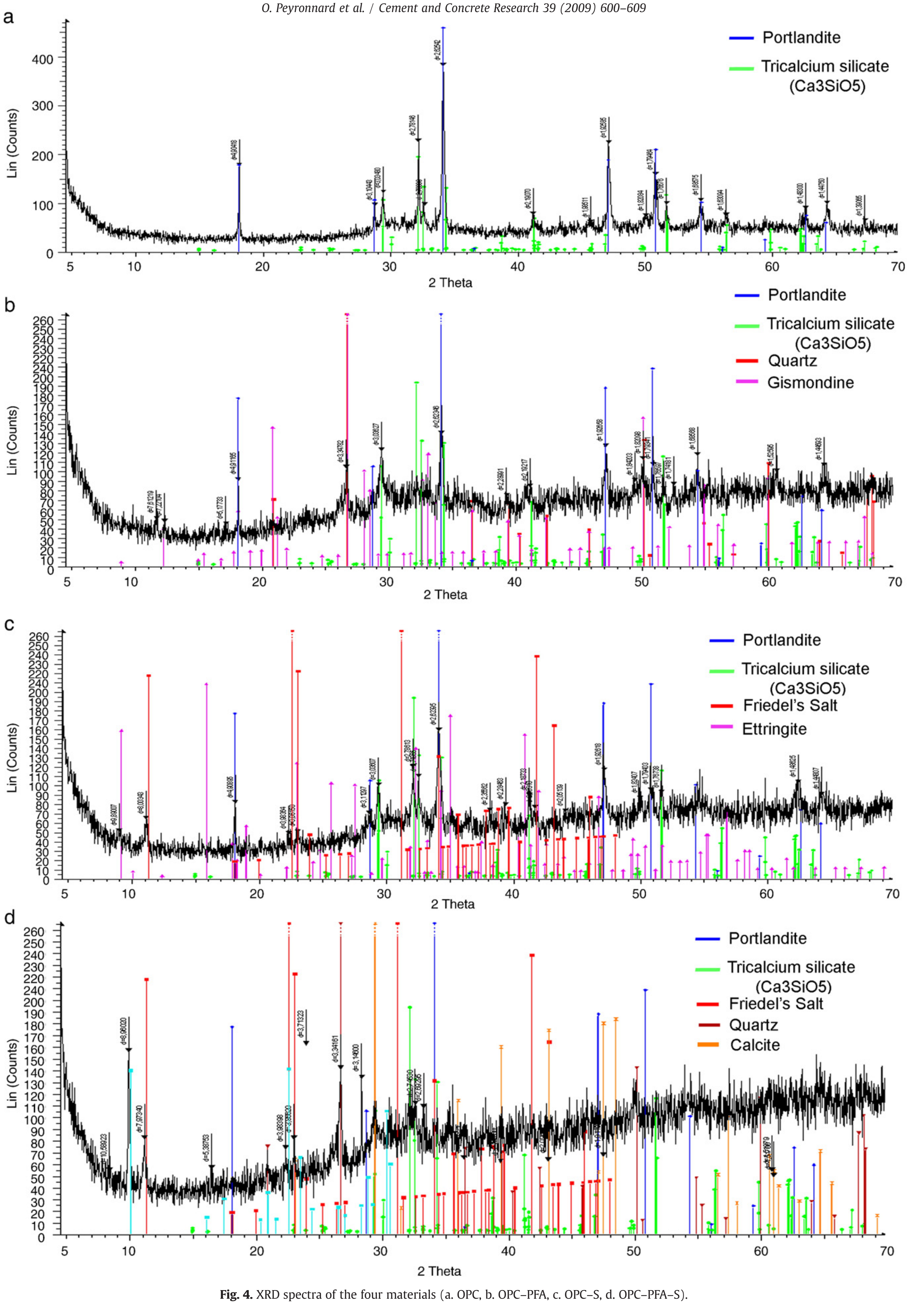

**Fig. 4.** XRD spectra of the four materials (a. OPC, b. OPC–PFA, c. OPC–S, d. OPC–PFA–S).

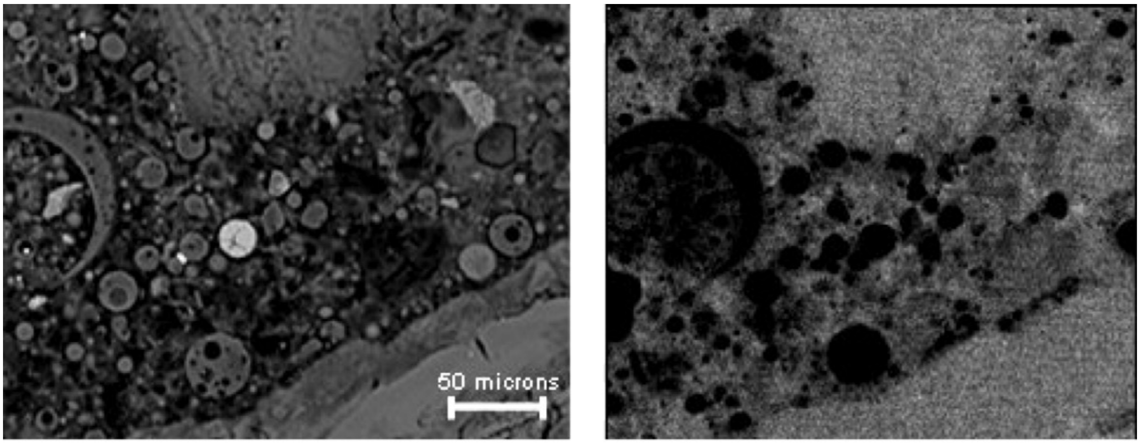

**Back Scattered Electrons image** **Calcium Map (line K)**

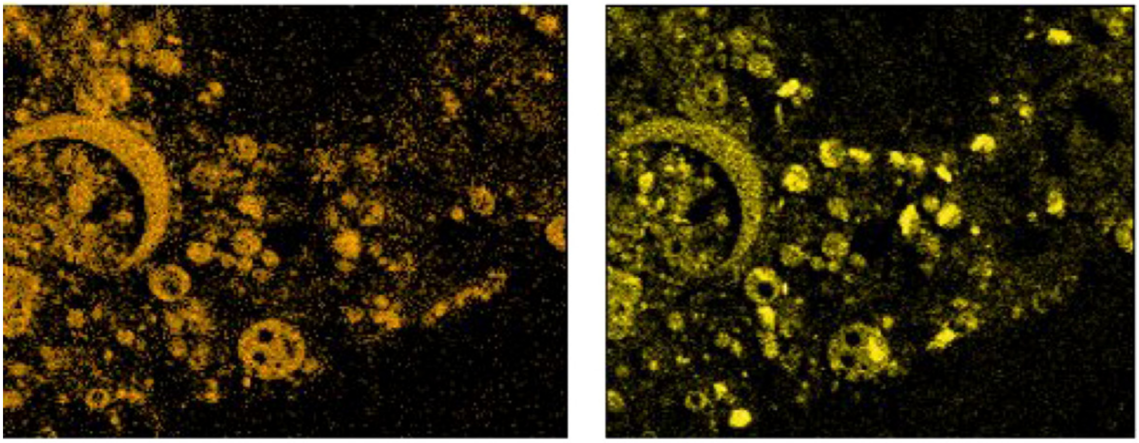

**Aluminum Map (line K)** **Silicon Map (Line K)**

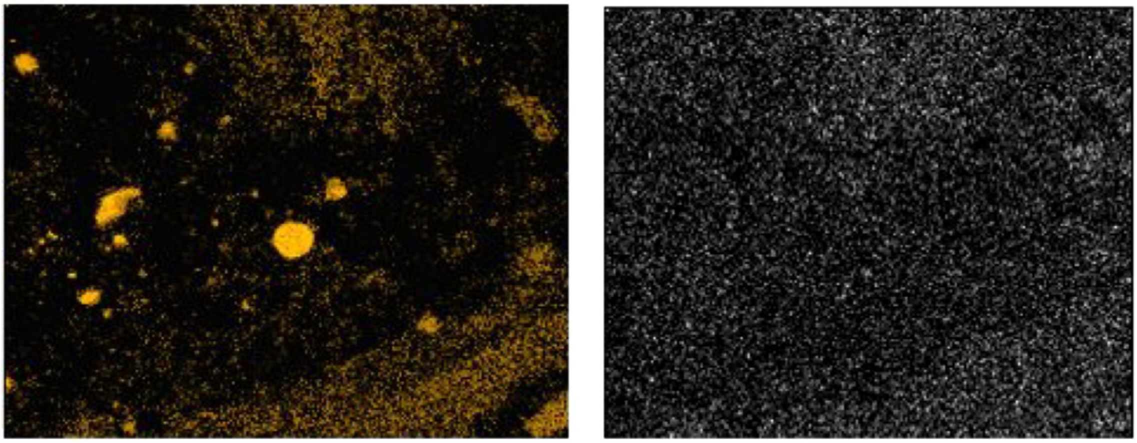

**Iron Map (Line K)** **Zinc Map (Line K)**

**Fig. 5.** Back Scattered Electron image and X-mapping in the core of OPC–PFA–S.

With an increase for pH under 10.2, the release of chromium appears as linked to sulfate one. The hypothesis of a substitution of sulfate by chromate in AFt or AFm phases can explain this phenomenon. Indeed, sulfates can be, in these phases, substituted by heavy metals oxyanions ($CrO_4^{2-}$, $AsO_4^{2-}$…), so they play an important role in heavy metal retention [13,17,21,22]. For OPC–PFA–S, the leaching of chromium decreases between natural pH and pH around 11.5 due to its probable occurrence as AFt (Cr-Ettringite).

The behavior of zinc is dependent of the nature of the binder and of the presence of sludge. Indeed when pure cement is used as binder (OPC and OPC–S), the release of zinc decreases for pH between 12.7 and 11.5, whereas it remains weak for binders containing fly ashes (OPC–PFA and OPC–PFA–S). Furthermore, the leaching of zinc is maximal for pH around 11 for the two materials without sludge (OPC and OPC–PFA) whereas it remains weak for OPC–S and OPC–PFA–S. The behavior observed for OPC and OPC–PFA, can be explained by the dissolution of a zinc phase, that could be calcium hydroxizincate [16], immediately followed by the setting up of another retention mechanism: precipitation as hydroxyde or adsorption on the surface of C–S–H [19,20].

### 3.3. Mineralogical study

The interpretation of XRD spectra (Fig. 4) is fairly complex because of an important background noise due to the large amount of amorphous phases in cementitious matrixes (C–S–H) and a too short scan time. Nevertheless, these XRD analyses reveal:

- the presence of portlandite and unhydrated $C_3S$ in the four materials;
- the presence of quartz and gismondine in OPC–PFA and OPC–PFA–S. These two phases, coming from fly ashes, are probably inert to the leaching processes because of their low solubility.
- the presence of Friedel's salt in OPC–S and OPC–PFA–S;
- the presence of ettringite in OPC–S.

Ettringite results from the hydration of aluminates present in Portland cement and fly ashes in presence of sulfates coming from cement (around 1.9%) and sludge (around 4.4%). Varying from 1.25% for OPC–PFA to 2.23% for OPC–S, the total content of sulfate in the four studied materials is sufficient to envisage the formation of ettringite. The precipitation of Friedel's salt in OPC–S and OPC–PFA–S is possible because of the high amount of chloride provided by the sludge. Indeed, being synthesized using ferric chloride, sludge contains around 6.2% of chloride.

The localization of elements in the matrix was studied through X-ray mapping and point analyses. Fig. 5 presents, as example, the elemental distributions through a zone observed in the core of OPC–PFA–S. Observations made on OPC–PFA and OPC–PFA–S show the presence of spherical alumino-siliceous particles corresponding to unhydrated fly ash particles (Fig. 5). Therefore, a fraction of the fly ash doesn't participate to the hydration reactions. Moreover, these fly ash particles can be observed in the leached and the unleached parts of the samples without any remarkable evolutions of their morphology or their composition. So, PFA particles can be considered as inert to the leaching process (in the “soft” conditions of the monolith leaching test).

The cement linking the particles (sludge, fly ash…) is mainly composed of calcium and silicon, and also contains some aluminum. This observation was predictable since this cement is composed of cementitious hydrates: Portlandite, C–S–H, AFt/AFm phases… Nevertheless, sulphur has not been localized in the matrixes due to a too weak signal. So, despite that a fraction of aluminum is probably precipitated as ettringite or monosulfoaluminate, aluminum is also present as other minerals: other AFt/AFm, hydrogarnets…

In OPC–S and OPC–PFA–S, observations also show some particles mainly composed of iron corresponding to sludge particles. These particles are also enriched in zinc and contained calcium and silicon. Observations conducted in the leached zone show that the leaching mainly induces a decalcification of these sludge particles. Therefore the presence of calcium, and silicon in these particles is probably due to their diffusion and precipitation as cementitious hydrates (portlandite, C–S–H…) in the pores of sludge particles. SEM observations also show the presence of grains of unhydrated cement in the matrixes (Fig. 6). This partial hydration of the binders is due to an inhibition of the hydration reaction caused by the constituents of sludge and/or ashes, in particular zinc. Indeed, the inhibition of cement hydration by zinc is generally explained by the formation of an impermeable layer composed of zinc hydroxide ($Zn(OH)_2$) [18,19] or calcium hydroxizincate ($CaZn_2(OH)_6$, $2H_2O$) [16] at the surface of $C_3S$ and $C_2S$ grains. The role of zinc in this inhibition is confirmed by its enrichment in the hydrated layer surrounding the unhydrated grains (Table 3).

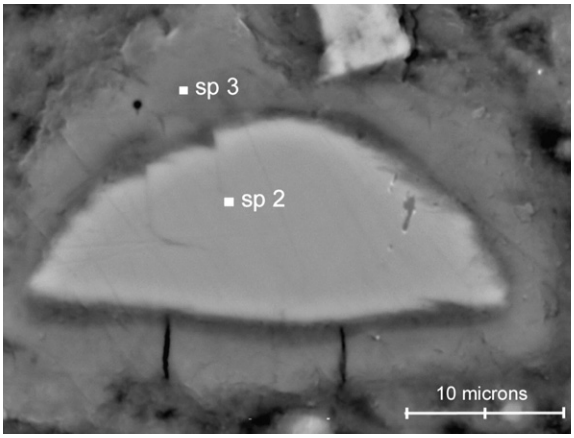

**Fig. 6.** Back Scattered Electron image of an unhydrated cement grain in OPC–S.

**Table 3**
Oxide weight percentage quantified from X-ray spectra obtained at the point noted sp2 and sp3 on Fig. 6.

| | sp2 | sp3 |
|---|---|---|
| $Fe_2O_3$ | 1.08 | 2.06 |
| $CrO_4$ | 0.58 | 0.78 |
| CaO | 79.73 | 65.68 |
| $TiO_2$ | 0.44 | 0.49 |
| $Al_2O_3$ | 0 | 0 |
| $SiO_2$ | 17.78 | 23.35 |
| $SO_4^{2-}$ | 0 | 0 |
| MgO | 0.14 | 0.38 |
| ZnO | 0.25 | 7.26 |
| Total | 100 | 100 |

Quantification made using a Phi-Rho-Z model.

Investigations made on zinc reveal a dispersion trough the matrix with an enrichment in sludge particles (Fig. 5). This localization is explained by the dissolution of the zinc hydroxide present in the sludge during the mixing of the pastes due to the highly alkaline pH. Two hypotheses can be given to explain zinc localization: it is adsorbed on the surface of C–S–H [19,20] or it precipitate as hydroxide or calcium hydroxizincate with the decrease of the water content caused by the hydration reactions.

## 4. Discussions: confrontation between differential acid neutralization analysis, leachates analysis and mineralogical study

The comparison of results of XRD analysis, SEM observations, differential acid neutralization analysis spectra and leaching of elements permits to establish advanced hypothesis on the nature of the reactive phases present in the unleached materials.

For the four pastes, the peak appearing, on differential analysis spectra, for a pH around 12.1 (between 12 and 12.2) is caused by the dissolution of portlandite. Indeed, the presence of portlandite is revealed by XRD and it is well known as instable for pH lower than 12.

Except for OPC–PFA–S, the release of silicon slightly increases from natural pH to a pH around 10–10.5, where a significant increase is observed. This behavior can be explain by the dissolution of C–S–H: decalcification for the highest pH and, then, dissolution of the siliceous matrix when the pH decrease under 10, resulting into the peaks observed for pH below 10–10.5. The slight increase, for higher pH, can be explained by the beginning of C–S–H incongruent dissolution. For OPC–PFA–S, the high solubility of silicon in basic condition could be explained by the presence of unhydrated cement. Indeed, unhydrated grains of cement were observed by SEM. The silicon, liberated by this dissolution, probably reprecipitates explaining the leaching decrease.

For each paste, two series of peaks are caused by the dissolution of the minerals containing aluminum and/or iron: peaks occurring for pH around 11.5–11.4 and peaks obtained for pH between 10 and 11. Various cementitious hydrates containing aluminum or iron can be form during the hydration: AFt/AFm phases, hydrogarnets… For these peaks, the absence of correlation between Al (Fe) and $SO_4^{2-}$ mobilization shows that Al (Fe) is present not only as ettringite (Fe-Ettringite) or monosulfoaluminate (monosulfoferrite) but also as hydrogarnets or carbonated AFt/AFm. This presence of unsulfated aluminates is confirmed by SEM-EDS observations.

Nevertheless, XRD diagrams show the presence of ettringite in OPC–S, and the high release of aluminum and sulfates in highly alkaline conditions observed for OPC–S and OPC–PFA–S can be explained by the solubility of ettringite. This higher sulfate for high pH release is not observed for the two binders (OPC and OPC–PFA), the monosulfoaluminates (and monosulfoferrites) being less soluble than ettringite (Fe-ettringite) for alkaline conditions, sulfates are probably present as AFm in these two pastes.

Finally, decreases of Al and Fe releases can be observed when the pH decreases fewer than 11. This behavior is due to their precipitation, probably as hydroxides.

A punctual increase of zinc release can also be observed for OPC and OPC–PFA. For OPC–PFA, this increase is correlated with the narrow peak observed at pH around 11.1. The leached zinc immediately reprecipitates or is, immediately absorbed on C–S–H. SEM-EDS observations show a correlation between zinc and other hydration products localization, in particular in the hydrated ring surrounding unhydrated cement grains. The leaching behavior of zinc can be explained by the dissolution of calcium hydroxizincate when the pH decreases around 11.1, and the setting of another retention mechanism: adsorption on C–S–H or precipitation as hydroxide. When the pH decreases below 10, zinc is released because of its desorption or the dissolution of zinc hydroxide.

For the four pastes, the chromium is released simultaneously of the mobilization of sulfate. Therefore, chromium is probably present as AFt or AFm phase due to a substitution of sulfates by chromates in those minerals. This hypothesis has not been confirmed by the mineralogical study, but is baked up by the observation of ettringite on XRD diagram.

Finally, the release of chloride increase in the first time of the acidification (pH between 13 and 11) in particular for OPC–S and OPC–PFA–S. XRD diagrams reveal the presence of Friedel's salt in these two materials. So the observed release is explained by the dissolution of this hydrated mineral.

Numerous hypotheses on links between mineralogy and leaching behavior can be establish from the confrontation of the results of the experiments performed (SEM-EDS, XRD, differential acid neutralization analysis and chemical analysis of selected leachates). Nevertheless, these hypotheses remain hardly confirmable due to the complexity of the studied materials. In a part II of this paper, we propose to use geochemical modeling and numerical simulation to test the hypotheses and establish a model of the leaching behavior of the studied materials.

## 5. Conclusions

In this work, the mineralogy and its links with the leaching behavior of stabilized/solidified synthetic hydroxide sludge were analyzed by coupling differential acid neutralization analysis, chemical analysis of selected leachate and a short mineralogical study by XRD and SEM-EDS.

The leaching of hydroxides sludge stabilized/solidified by Portland cements is controlled by the dissolution of various minerals:

At the beginning of leaching process, the pH is maintained up to 12 by the dissolution of portlandite. Due to pozzolanic reactions and/or hydration inhibitions, cement pastes containing sludge and/or PFA have fewer portlandite amounts and therefore a weaker acid neutralization capacity. For pastes having a high chloride content (OPC–S and OPC–PFA–S), chloride form Friedel's salt that, also, dissolves at high pH.

For pH between 12 and 10, the leaching is mainly controlled by the dissolution of aluminates and ferrites, probably AFt/AFm and/or hydrogarnets. The nature of these hydrated phases can't be precisely identified. However, it is shown that AFt and AFm appear not only as ettringite and monosulfloaluminate, but also as unsulfated forms.

For lower pH (<10) the leaching behavior is controlled by the dissolution of an alumino-sulfated mineral, probably ettringite and the dissolution of the siliceous matrix of C–S–H. The observed decrease of aluminum and iron release shows their reprecipitation, probably as hydroxide.

Zinc behavior is controlled by two distinct phases: dissolution of calcium hydroxizincate for a pH around 11.1 and reprecipitation as hydroxide or adsorption on C–S–H of the zinc released. The release of chromium is linked to those of sulfates due to a substitution of sulfate by chromate in AFt (ettringite) and AFm (monosulfoaluminate).

The presented approach, coupling differential acid neutralization analysis, chemical analysis of selected leachates and mineralogical study, appears highly pertinent to characterize the leaching behavior of a cementitious matrix and its links with its mineralogy. Nevertheless, the hypothesis formulated remains imprecise (e.g. nature of AFm/AFt) and hardly confirmable. To improve the experimental results some modifications can be made to the protocol:

- The range of pH scanned during the acid neutralization test should be increased for pH lower than 9, in order to highlight dissolution/precipitation reactions occurring, and in particular segregate the dissolution of ettringite and of C–S–H siliceous matrix;
- For each observed peaks, two leachates (before and after the peak) should be analyzed to facilitate the identification of the dissolving minerals and of the elements, in particular pollutants, having a behavior independent to the main component one;
- The XRD must be made with a higher scan time. An XRD analysis could, also, be performed on the filtration cake corresponding to the analyzed leachates.

Besides, geochemical modeling can be used to test the pertinence of the formulated hypothesis to describe the leaching behavior. In the part II of this paper, we propose to use geochemical modeling and numerical simulation as an aid tool for the identification of the hydrated minerals controlling the leaching behavior of the for studied cement pastes.

## References

[1] AFNOR NF EN 12920: Caractérisation des déchets - Méthodologie pour la détermination du comportement à la lixiviation d'un déchet dans des conditions spécifiées. 2006.

[2] ADEME. Evaluation de l'écocompatibilité de scénarios de stockage et de valorisation des déchets. ADEME Editions, collection: Connaître pour Agir, 2002, 148 p.

[3] C.E. Halim, S.A. Short, J.A. Scott, R. Amal, G. Low, Modelling the leaching of Pb, Cd, As, and Cr from cementitious waste using PHREEQC, Journal of Hazardous Materials A215 (2005) 45–61.

[4] G.K. Glass, N.R. Buenfeld, Differential acid neutralisation analysis, Cement and Concrete Research 29 (1999) 1681–1684.

[5] J.A. Stegemann, R.J. Caldwell, C. Shi, Response of various solidification systems to acid addition, in: J.J.J. Goumans, G.J. Senden, H.A. van der Sloot (Eds.), Waste Materials in Construction: Putting Theory into Practice, Studies in Environmental Science, vol. 71, Elsevier Science, Amsterdam, 1997, pp. 803–814.

[6] J.A. Stegemann, C. Shi, Waste acid resistance of different monolithic binders and solidified wastes, in: J.J.J. Goumans, G.J. Senden, H.A. van der Sloot (Eds.), Waste Materials in Construction: Putting Theory into Practice, Studies in Environmental Science, vol. 71, Elsevier Science, Amsterdam, 1997, pp. 551–562.

[7] G.K. Glass, B. Reddy, N.R. Buenfeld, Corrosion inhibition in concrete arising from its acid neutralization capacity, Corrosion Science 42 (2000) 1587–1598.

[8] G.K. Glass, B. Reddy, N.R. Buenfeld, The participation of bound chloride in passive film breakdown on steel in concrete, Corrosion Science 42 (2000) 2013–2021.

[9] E. Fried, M. Benzaazoua, B. Bussière, T. Belem, Study of the leaching behaviour and metal fixation within cemented paste backfill materials, 9th International Symposium in Mining with Backfill. Organized by the Canadian Institute of Mining, Metallurgy and Petroleum (CIM), Montreal, Quebec, Canada, April 29-May 2, 2007.

[10] O. Peyronnard. Apports méthologiques pour la modélisation du comportement à la lixiviation de résidus minéraux. Applications aux solidifiats de boues d'hydroxydes métalliques. Ph.D. Thesis INSA de Lyon, 2008.

[11] F.P. Glasser, Fundamental aspects of cement solidification and stabilization, Journal of Hazardous Materials 52 (1997) 151–170.

[12] J.D. Ortego, Y. Barroeta, F.K. Cartledge, H. Akhter, Leaching effects on silicate polymerization. An FTIR and Si-NMR study of lead and zinc in Portland cement, Environmental Science and Technology 25 (1991) 1171–1174.

[13] J.N. Diet, Stabilisation/Solidification des déchets: Perturbation de l'hydratation du ciment Portland par les substances contenues dans les boues d'hydroxydes métalliques. Ph D Thesis, INSA de Lyon, 1996.

[14] D. Stephen, R. Mallman, D. Knöfel, R. Härdtl, High intakes of Cr, Ni and Zn in clinker. Part II: influence on the hydration properties, Cement and Concrete Research 29 (1999) 1959–1967.

[15] U.A. Birnin-Yauri, F.P. Glasser, Friedel's salt, $Ca_2Al(OH)_6(Cl,OH)\ 2H_2O$: its solid solutions and their role in chloride bonding, Cement and Concrete Research 28 (12) (1998) 1713–1723.

[16] V.A. Rossetti, F. Medici, Inertization of toxic metals in cement matrices: effects on hydration, setting and hardening, Cement and Concrete Research 25 (1995) 1147–1152.

[17] M. Chrysochoou, D. Dermatas, Evaluation of ettringite and hydrocalumite formation for heavy metal immobilization: literature review and experimental study, Journal of Hazardous Materials 136 (2006) 20–33.

[18] G. Arliguie, J.P. Ollivier, J. Grandet, Etude de l'effet du zinc sur l'hydratation de la pâte de ciment Portland, Cement and Concrete Research 12 (1982) 79–86.

[19] A. Stumm, K. Garbev, G. Beuchle, L. Black, P. Stemmermann, R. Nüesch, Incorporation of zinc into calcium silicate hydrates, part I: formation C–S–H with C/S = 2/3 and its isochemical counterpart gyrolite, Cement and Concrete Research 35 (2005) 1665–1675.

[20] X.D. Li, Y.M. Zhang, C.S. Poon, I.M.C. Lo, (2001.a) Study of zinc in cementitious material stabilised/solidified wastes by sequential chemical extraction and microstructural analysis, Chemical Speciation and Bioavailability n° 13 (1) (2001).

[21] T. Phenrat, T.F. Marhaba, M. Rachakornkij, A SEM and X-ray study for investigation of solidified/stabilized arsenic-iron hydroxide sludge, Journal of Hazardous Materials B118 (2005) 185–195.

[22] T. Matschei, B. Lothenbach, F.P. Glasser, The AFm phase in Portland cement, Cement and Concrete Research 37 (2007) 118–130.